Iranian Journal of Science and Technology, Transactions of Electrical Engineering (2020) 44:849–860
https://doi.org/10.1007/s40998-019-00274-8

RESEARCH PAPER

# Presenting New Triple Methods for Fault Detection, Location, and Its Identification in DC Microgrid

R. Eslami[1] · S. A. Hosseini[2]

Received: 23 March 2019 / Accepted: 17 September 2019 / Published online: 24 September 2019


**Abstract**

Unlike conventional AC systems, the DC systems cannot sustain high-magnitude fault currents. Therefore, detection, location, and identification of faults are the issues of great importance. On this basis, in this paper, three methods are investigated to detect a fault and determine its exact location and its type in DC microgrids. A module is installed at the beginning and end of all grid lines to implement the proposed method. Modules provide current and voltage sample signals and using the proposed triple algorithms analyze these signals online. Accordingly, modules use current amplitude, voltage amplitude, and current differential to detect fault occurrence. After detecting a fault, fault location algorithm activates to determine the fault location. On this basis, modules which have detected the fault use the fault current direction to determine its location. In the proposed fault-type identification algorithm, its type is identified by modules that detect the fault using the voltage drop that is caused by the fault. The proposed triple methods are implemented on two sample DC microgrids in DIgSILENT software. The results prove that the proposed method is capable of determining the occurrence of all types of DC faults, their exact location, and their identification considering structural uncertainties of the network. In addition, the proposed method can discriminate between transient and permanent faults with high accuracy.

**Keywords** DC microgrid · Fault detection · Fault location · Fault identification · Uncertainty

## 1 Introduction

Many factors such as progress in power electronic devices technology, increasing of DC consumers, interests of using renewable distributed generations (RDG), and improvement in control methods of these resources have caused increment trend to DC microgrids (Mohanty and Pradhan 2018; Howlader et al. 2018). However, the application of these microgrids is still in laboratory dimensions due to the protection issues that these microgrids encounter (Lv et al. 2018).

✉ R. Eslami
eslami@sut.ac.ir

S. A. Hosseini
hosseini.amir@gut.ac.ir

[1] Faculty of Electrical Engineering, Sahand University of Technology, Tabriz, Iran

[2] Department of Electrical Engineering, Golpayegan University of Technology, Isfahan, Iran

In addition to lack of experience, standards, and enough guidelines in the field of DC microgrids protection, fault detection challenge is the most important problem of DC microgrids protection (Hosseini et al. 2016). The main challenge in fault detection of these networks is due to the fault current shortage (Nimpitiwan et al. 2007). Actually, DC microgrids are equipped with power electronic devices and inverter-based DG resources that allow supplying maximum fault current only 2–3 times than nominal current. This amount of current is too low for fault detection (Hosseini et al. 2016). Structural uncertainty of microgrid causes more complexity in fault detection of DC microgrids (Hassan et al. 2018). Actually, microgrids do not have a constant topology and their topology is changed due to connecting and disconnecting of DGs and lines and also operational mode of microgrids (normal or islanding modes) (Hosseini et al 2018a, b). Therefore, any protection method presented for DC microgrids should be able to detect all possible faults in these networks despite structural uncertainties of these networks.

Generally, there are two kinds of faults in DC microgrids which are pole-to-pole and pole-to-ground faults (Salomonsson et al. 2009). Although the presented method in some studies such as Lv et al. (2018) recognize only one of the fault types, the suggested method in many studies can recognize both fault types. Most of these studies (which could detect two kinds of faults in DC microgrids) such as Park and Candelaria (2013), Aswani and Kanakasabapathy (2016) have used the current differential to detect a fault. The long required time to detect a fault and finding an exact threshold value considering network dynamic changes are challenges of the current differential methods (Abdali et al. 2019). In order to improve the speed of differential protection in the process of fault detection in DC microgrids, the simultaneous use of this method together with fuzzy controller is proposed in Abdali et al. (2019). Similarly, simultaneous using of differential method as the main protection and voltage drop protection is proposed in Ming et al. (2016) for a ring DC microgrid based on wind turbines. However, using voltage analysis is proposed alone in some studies (such as Wen and Weiqiang 2016; Balasreedharan and Thangavel 2016; Zhao et al 2016) for fault detection. In these studies, voltage variations slope ($^{dv}/_{dt}$) is used to detect the fault. Similarly, the use of current magnitude is suggested in Shabani and Mazlumi (2019) for protecting DC microgrids. However, in the proposed method in Shabani and Mazlumi (2019), extended communication links are used in the protection process. In order to increase selectivity to detect the fault, Mohanty and Pradhan (2017) present the hybrid method. In the proposed hybrid method, voltage variation slope and current variation slop ($^{di}/_{dt}$) are simultaneously monitored to detect a fault in DC microgrid. Other hybrid methods are presented in Abdali et al. (2017) that is based on both current differential and $^{di}/_{dt}$, in Jamali et al. (2018) where fault detection is done through the first and second derivatives of the current, and in Amamra et al. (2017) where it is done via current having noise and $^{di}/_{dt}$.

Most of the presented methods are able to detect the fault in the network and cannot detect its exact location and type. On the other hand, microgrids structural uncertainty is ignored in almost all of the investigated studies. Based on variations of fault current amplitude in various topologies of the network, especially between operation topologies in islanding and normal modes, ignoring uncertainties of network structure can cause reliability reduction in the proposed protection methods (Hosseini et al. 2016; Eslami et al. 2017).

The most appropriate method for responding to microgrids structural uncertainties is known as the adaptive protection (Basak et al. 2012). Accordingly, Dhar et al. (2017, 2018), Meghwani et al. (2017) propose adaptive methods to detect a fault in DC microgrids. In these methods, adaptive threshold values have been used. For this purpose, all microgrid operational topologies are identified and a threshold value is calculated and saved as offline for each topology. In each topology of microgrid, the specific threshold is called from memory and is used as protection system settings till the structure is validated. Requiring a lot of free memory to save network topologies settings and inability to predict all the network topologies are challenges that are posed in methods using offline settings (Conti and Nicotra 2009; Conti 2009). So using an online adaptive method that can detect all possible faults based on DC microgrid structural uncertainties is required.

Accordingly, triple methods are presented in this article to detect faults, determine its occurrence location, and identify its type. The proposed methods operate according to the received samples of the network voltage and current signals. Modules which are located at the beginning and the ending of all microgrid lines receive and analyze signals. Modules use current amplitude, voltage amplitude, and current differential parameters in the proposed fault detection algorithm. If according to some consecutive samples a fault was observed, this issue would be notified to the central server by communications links between each module and the central server. After detecting a fault, the proposed algorithm is activated to detect its location. Accordingly, modules which detected the fault determine its occurrence location by using the direction of fault current. Then, the third algorithm, fault-type identification algorithm, is activated. This algorithm identifies the fault type (pole to pole or pole to ground) based on the amount of voltage drop. All operational topologies of the microgrid can protect online by the proposed methods. Also, based on designed mechanisms in the proposed fault detection algorithm, this algorithm can discriminate network transients and permanent faults. Accordingly, during transients which are usually generated by switching in the network, the protection system does not operate by mistake. The proposed method is implemented on two sample DC microgrids in DIgSILENT software. Results prove the ability of the proposed method in detection, location, and identification different types of faults considering structural uncertainties in DC microgrids.

The structure of the paper is as follows. In Sect. 2, the shortcomings of the proposed methods in similar studies are investigated. In Sect. 3, the proposed triple methods of this paper are presented to detect a fault, determine its location, and its identification in DC microgrids. In Sect. 4, the proposed triple methods are implemented on two sample microgrids in different operational topologies and the results are analyzed.

## 2 Problem Statement

As investigated in the previous section, most studies use current differential or current variations slope to detect a fault and its location. In this section, these methods' shortcomings to detect the fault occurrence and its exact location are presented by analyzing them on a case study of sample microgrid of Fig. 1. This microgrid was used as a case study in Jae-Do et al. (2013).

To evaluate, the recorded signals of the currents $I_{16}$ and $I_{18}$ and also $I_{11}$ and $I_{13}$ for occurred fault in point $F$ are shown in Figs. 2 and 3, respectively.

As shown in Fig. 2, since during a fault, the DG1 increases the fault current, current $I_{18}$ is amplified significantly by DG1 current ($I_{17}$) and current $I_{16}$ will be created as a result. On the other hand, if a fault occurred behind a module, the module current direction will be changed due to the fault current (Jae-Do et al. 2013). Thus, current $I_{13}$ had fed DC load, when a fault occurs behind it, as shown in Fig. 3, in addition to the increase in its magnitude, its direction would also change and would flow toward fault.

If the current differential was used to detect a fault in microgrid of Fig. 1, this fault would be detected between $I_{11}$ and $I_{13}$ and also between $I_{16}$ and $I_{18}$. However, such a fault detection is wrong. Even if the method of current variations slope was used, based on the presented signals in Figs. 2 and 3, fault occurrence would be detected in two mentioned parts.

Therefore, it is clear that the previous methods have problems for detecting a fault location. In addition, many of these methods cannot detect fault exact type. On the other hand, inattention to microgrid structural uncertainties and inability to create a distinction between transient states and permanent faults are such cases that cause the proposed methods in previous studies to face serious challenges. Therefore, developing a comprehensive method to detect a fault, determine its location, and its identification in DC microgrids is necessary.

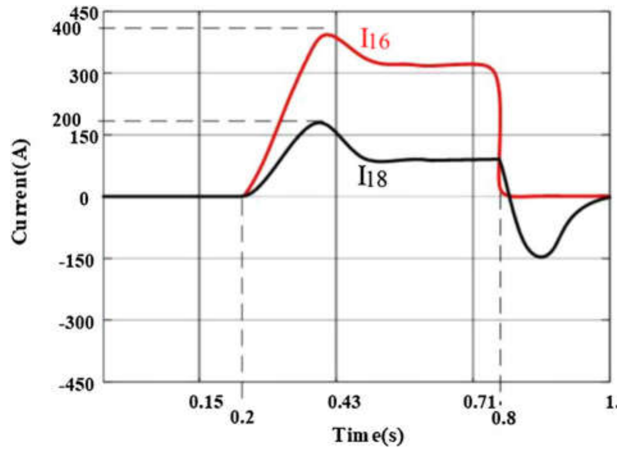


**Fig. 2** Current waveforms ($I_{16}$ and $I_{18}$) in microgrid of Fig. 1 during fault $F$

**Fig. 1** Sample network for analyzing previous studies

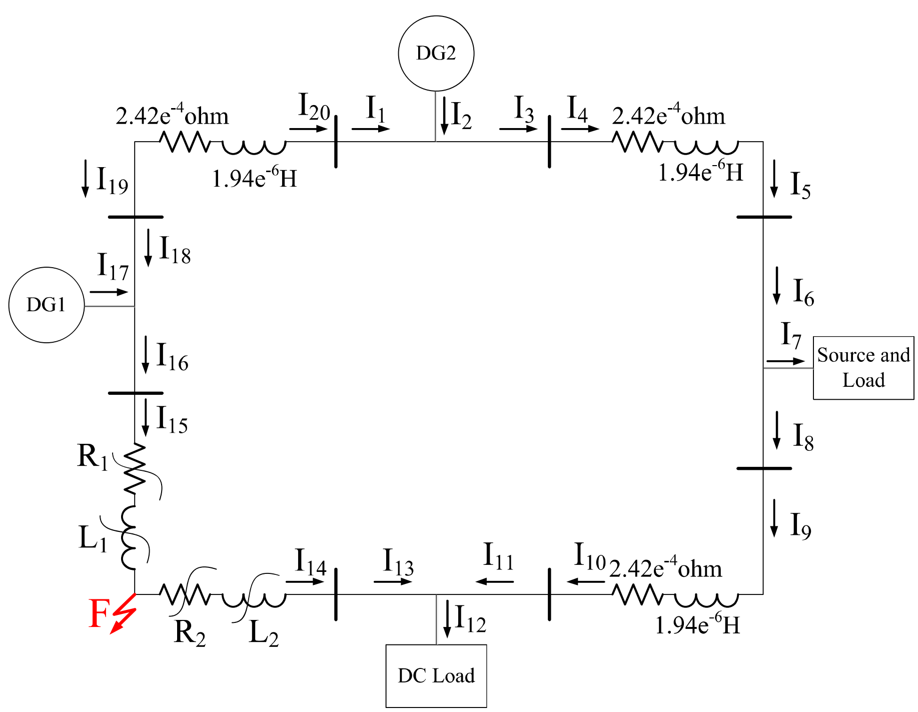

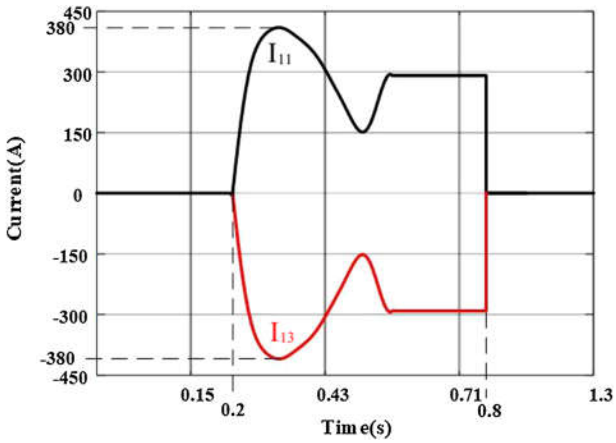


**Fig. 3** Current waveforms ($I_{11}$ and $I_{13}$) in microgrid of Fig. 1 during fault $F$

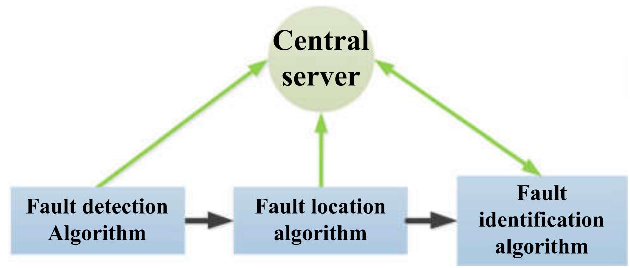


**Fig. 5** Block diagram of the triple proposed methods

## 3 Proposed Method

Based on Fig. 4, to implement the proposed method, sensing modules are installed in two ends of all grid lines. Modules have to receive and analyze various electrical parameters of the network. Based on the received parameters, the proposed triple methods to detect a fault, determine its exact location, and identify its type are executed. Based on Fig. 5, these results are sent to the server through reliable communication links, which are between modules and the central server, in order to program the protection coordination process and fault clearance. Therefore, as it is obvious in the proposed method, the fault detection is done by the modules and the central server has the only role of establishing appropriate protection coordination. Thus, the reliability of this method is significantly higher than those in which the whole decision-making process is located in the central server. If communications are created between the whole modules on the network, the implementation of the proposed method could be completely decentralized.

It should be mentioned that the proposed fault detection method could be generalized and applied for other microgrid structures if the modules are set aptly in different parts of the microgrid for sampling voltage and current waveforms. Generally, to implement the proposed method, it does not matter what topology the microgrid has; what is important is that the necessary tools be suitably placed on the network for the implementation of the proposed method and then the different stages of the proposed method upon the studied network be carried out. By observing the following, the proposed fault detection method will correctly work on other networks as well.

### 3.1 Fault Detection Algorithm

All modules continuously sample voltage and current signals and investigate fault occurrence based on the proposed analysis in this section. In this plan, current amplitude per unit ($CA^{m}_{\text{p.u, sample } i}$), current differential per unit of each module and its adjacent modules ($CD^{m}_{\text{p.u, sample } i}$), and voltage per unit values ($V^{m}_{\text{p.u, sample } i}$) are electrical parameters that $m$th module extracts from the $i$th sample of voltage and

**Fig. 4** Required background to implement the proposed method

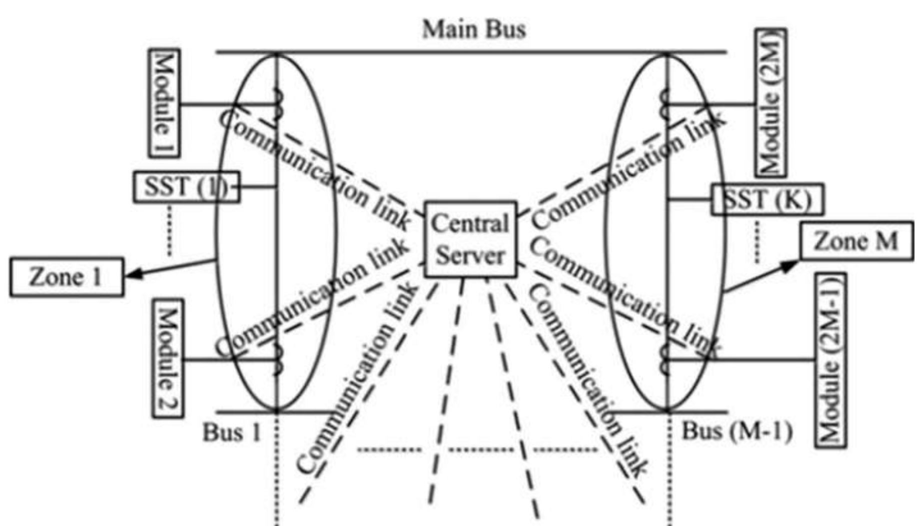

current signals to detect a fault. Assuming that $N$ samples are required to detect a fault by module $m$, so a $N$ member set is created for all involved parameters in fault detection process such as Eqs. (1)–(3).

$$\mathrm{CA}^{m}_{\mathrm{p.u}} = \left\{\mathrm{CA}^{m}_{\mathrm{p.u,sample\,1}}, \mathrm{CA}^{m}_{\mathrm{p.u,sample\,2}}, \ldots, \mathrm{CA}^{m}_{\mathrm{p.u,sample}\,N}\right\} \tag{1}$$

$$\mathrm{CD}^{m}_{\mathrm{p.u}} = \left\{\mathrm{CD}^{m}_{\mathrm{p.u,sample\,1}}, \mathrm{CD}^{m}_{\mathrm{p.u,sample\,2}}, \ldots, \mathrm{CD}^{m}_{\mathrm{p.u,sample}\,N}\right\} \tag{2}$$

$$V^{m}_{\mathrm{p.u}} = \left\{V^{m}_{\mathrm{p.u,sample\,1}}, V^{m}_{\mathrm{p.u,sample\,2}}, \ldots, V^{m}_{\mathrm{p.u,sample}\,N}\right\} \tag{3}$$

In these equations, $\mathrm{CA}^{m}_{\mathrm{p.u}}$ shows $\mathrm{CA}^{m}_{\mathrm{p.u,\,sample}\,i}$ set in obtained samples of current signal, $\mathrm{CD}^{m}_{\mathrm{p.u}}$ shows $\mathrm{CD}^{m}_{\mathrm{p.u,\,sample}\,i}$ set in obtained samples of current signal, and $V^{m}_{\mathrm{p.u}}$ is $V^{m}_{\mathrm{p.u,\,sample}\,i}$ set in obtained samples of voltage signal.

After receiving various samples of required electrical signals to detect a fault, module $m$ starts to detect fault based on Fig. 6 algorithm. On this basis, if current amplitude exceeds the defined threshold ($\mathrm{CA}^{m,\mathrm{TH}}$), current differential between $m$th module and its adjacent module will exceed the threshold value ($\mathrm{CD}^{m,\mathrm{TH}}$), and also voltage will exceed its threshold value ($V^{m,\mathrm{TH}}$); then, $m$th module will detect the fault. However, it would not notify the central server till the fault is remained for three consecutive samples (sample 1, sample 2, sample 3). Actually, the proposed method tries to separate permanent fault from transient states. Accordingly, the detection parameters are sampled consecutively, and the mentioned condition will only be realized if the number of predetermined parameter samples surpasses its threshold. Otherwise, the occurred condition is a temporary non-fault condition. This process can easily distinguish permanent faults from transient faults.

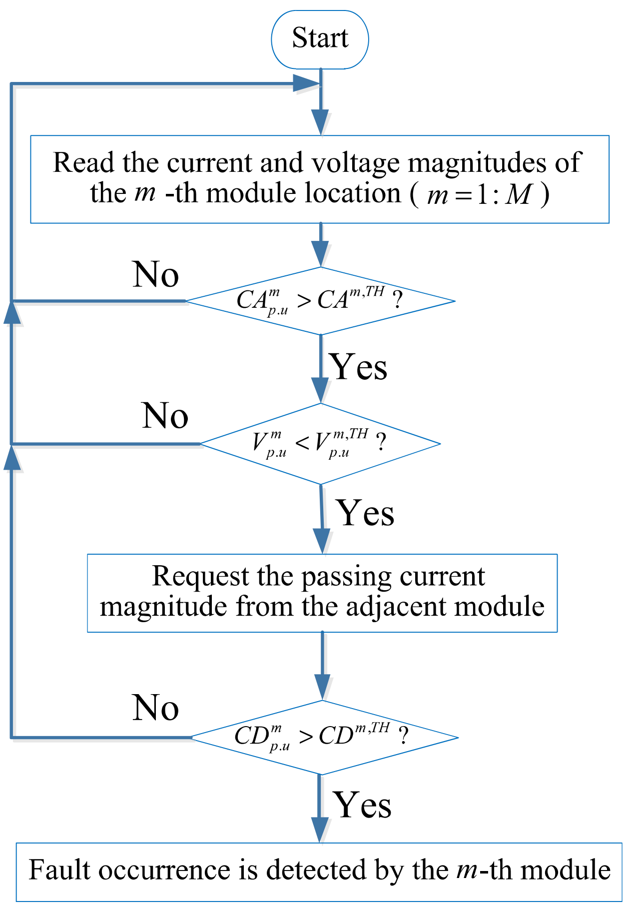


**Fig. 6** Proposed DC fault detection algorithm by each module

### 3.2 Fault Location Algorithm

After detecting a fault occurrence by some modules, its exact location has to be determined. As shown before, methods of current differential and slope of current variations over time might be inaccurate for identifying a fault location. Accordingly, this paper suggests a method in which the fault current direction is used to detect the fault location.

Based on the proposed algorithm in Fig. 7, current direction ($\mathrm{CS}^{m}$) is an appropriate criterion for identifying a fault location in modules that have detected a fault. Thus, if the current of this module and its adjacent module were between two modules, the fault location would be in area between two modules. It should be noted that if current from a module enters the area, $\mathrm{CS}^{m}$ will be considered positive and if passing current exits the area, $\mathrm{CS}^{m}$ will be considered negative for this module.

### 3.3 Fault-Type Identification Algorithm

According to Fig. 5, in the proposed method in this paper, after detecting fault location, its type is identified. Microgrid possible faults are whether pole-to-pole or pole-to-ground faults. In pole-to-ground faults, just the faulted pole is affected and this fault is almost affectless on the healthy pole (Salomonsson et al. 2009). Therefore, in this fault type, faulted pole is detected in the proposed method to minimize the outages and accordingly loads on the healthy pole are still being supplied.

Since the module which is nearest to a fault has the highest voltage drop [based on Salomonsson et al. 2009; Jae-Do et al. 2013], in order to identify the fault type, the module with the highest voltage drop (module $m'$) is identified and the proposed algorithm is presented to identify the fault type by this module. Equation 4 shows the method of identifying DC fault type by $m'$th module.

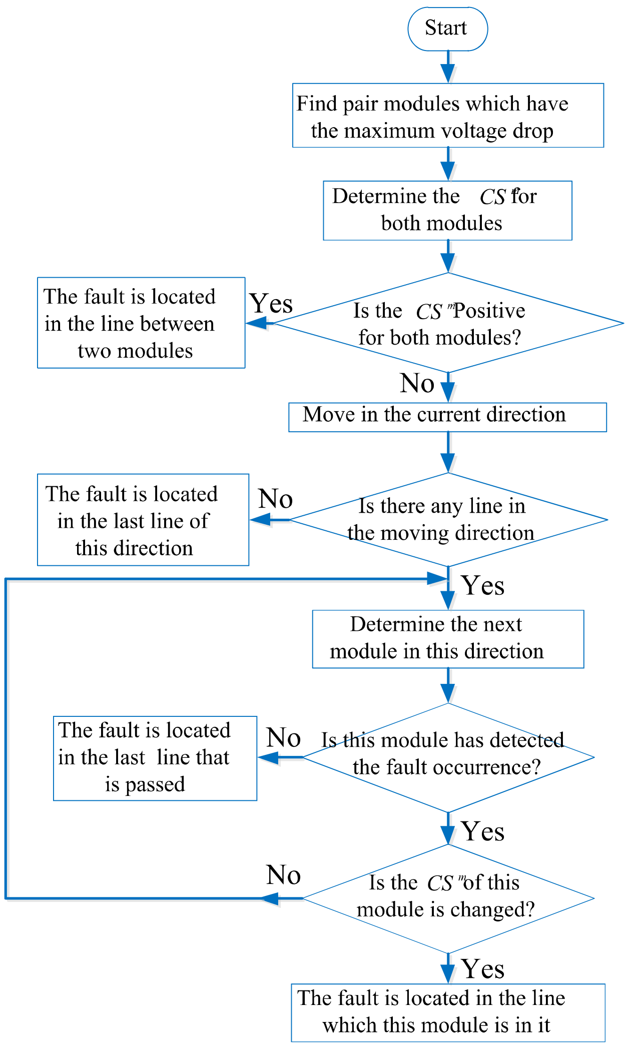


Fig. 7 Proposed DC fault location algorithm

$$\begin{cases} V^{m\prime}_{\text{p.u}} < 0.5\ \text{p.u} \Rightarrow & \text{Fault is pole to pole} \\ V^{m\prime}_{\text{p.u}} > 0.5\ \text{p.u} \Rightarrow & \begin{cases} V^{m\prime,+}_{\text{p.u}} > V^{m\prime,-}_{\text{p.u}} \Rightarrow & \text{Fault is in negative pole} \\ V^{m\prime,+}_{\text{p.u}} < V^{m\prime,-}_{\text{p.u}} \Rightarrow & \text{Fault is in positive pole} \end{cases} \end{cases} \quad (4)$$

According to Salomonsson et al. (2009), pole-to-pole faults are low impedance faults. Therefore, during a fault the voltage of two poles would be negligible (less than 0.5 per unit). While in pole-to-ground faults, since one pole is not faulty, the voltage between two poles (whether the fault is low or high impedance) will be more than 0.5 per unit. Therefore, fault type can be determined by calculating the voltage between two poles. Also, in pole-to-ground faults, the pole with less voltage amplitude is known as the faulted pole. On this basis, Fig. 8 shows the proposed algorithm to determine DC faults identification.

An important factor in every method for fault detection in power networks is time. In previous methods, fault detection happens after the sampling process. However, in the proposed method, process of voltage and current samples has been done in real time with obtaining the next samples. Accordingly, in the proposed method, the time of implementing the plan decreased compared to current popular methods. It should be mentioned that the time of implementing any fault detection methods also relies on the type of the microprocessor used in the module structure.

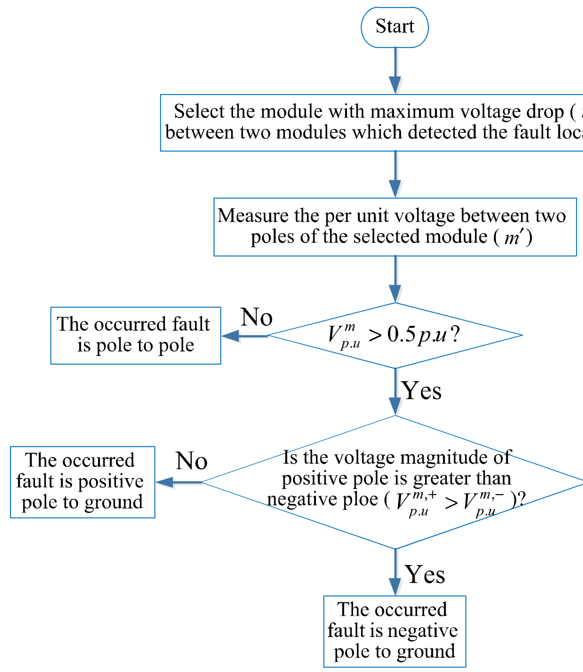


Fig. 8 Flowchart of fault identification algorithm

## 4 Simulation Results

### 4.1 Fault Detection in DC Ring Microgrids in Islanded Mode

To investigate the proposed triple methods in the islanded operation mode, these methods are implemented on a sample DC microgrid shown in Fig. 9. This microgrid had been used to implement the proposed method in Maqsood and Corzine (2016) earlier, and in this paper some changes are applied to it. Data associated with the sample microgrid of Fig. 9 are presented in Table 1. As it is clear, there are two DC distributed generation resources and two DC loads which are fed by a boost converter and an AC load which is fed by an inverter.

To obtain threshold values, similar to the method of AC fault detection in Eslami et al. (2017), the worst conditions that can challenge the proposed method are considered. Accordingly, in offline mode and before any event, the faults that have less values of detection parameters (depending on the fault type and closeness and remoteness of

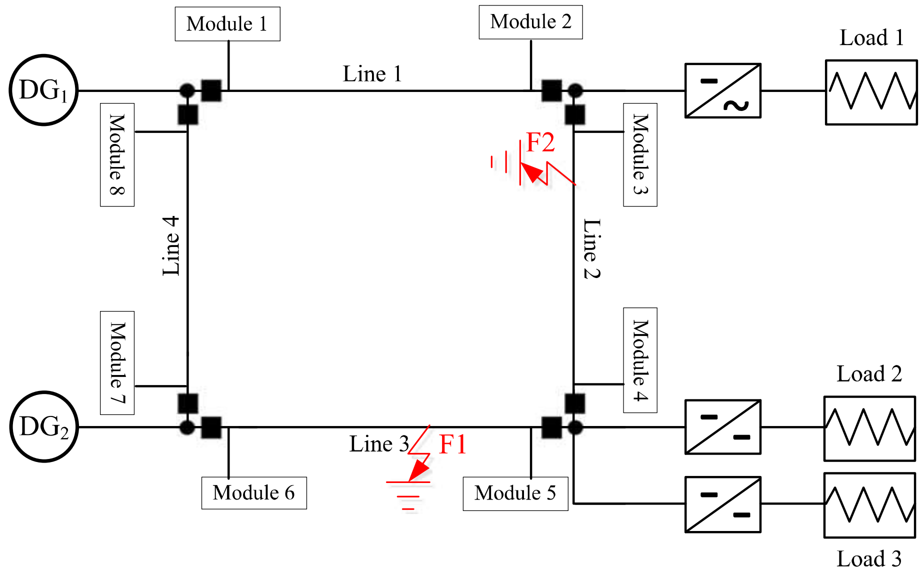


**Fig. 9** Sample DC microgrid to investigate the proposed methods in the islanded mode

**Table 1** Data of DC microgrid of Fig. 9

| Distributed generations | | | Loads | | Lines | |
|---|---|---|---|---|---|---|
| | | | | | $R$ = 2.42 × $10^{-4}$ Ω/km | $L$ = 1.94 × $10^{-6}$ H/km |
| Number | $R$ (Ω) | Voltage (V) | Number | Magnitude | Number | Length (km) |
| $DG_1$ | 1 | 400 | Load 1 | 50 Ω | Line 1 | 1 |
| $DG_2$ | 1 | 400 | Load 2 | 10 µF | Line 2 | 2 |
| | | | Load 3 | 100 Ω | Line 3 | 1.5 |
| | | | | | Line 4 | 3 |

the fault from the sources), and as well, non-faulty transient states that have the maximum detection values (depending upon the intensity of the generated variations in voltage and current signals) are detected and with regard to the fact that three detection parameters are considered, the thresholds of these three parameters are determined in a way that for all possible faults, these three conditions are met and the fault is detected correctly. Also, the threshold limits should be set so that for the stable transient states happened in the network, at least one of the three conditions is not satisfied and the occurred event correctly not be detected as fault. Accordingly, the threshold values $V^{m,\mathrm{TH}}$, $\mathrm{CA}^{m,\mathrm{TH}}$, and $\mathrm{CD}^{m,\mathrm{TH}}$ are calculated for various modules of sample microgrid equal to 0.8 p.u, 1.5 p.u, and 2 p.u, respectively.

It should be noticed that in all simulations on sample microgrids, three samples are used in a period of 100 ms for parameters $V^{m}_{\mathrm{p.u}}$, $\mathrm{CA}^{m}_{\mathrm{p.u}}$, and $\mathrm{CD}^{m}_{\mathrm{p.u}}$.

#### 4.1.1 Symmetric Fault Detection

To investigate the proposed method's ability to detect symmetric faults, a pole-to-pole fault with an insignificant fault resistance is located in point $F1$ of the microgrid in Fig. 9. Located modules in different points of the network are sampling voltage and current signals continually, and fault detection algorithm investigates collected information to detect possible faults based on Fig. 6. Table 2 shows the modules' required values before and after fault $F1$.

Based on Table 2, the recorded values in modules 5 and 6 for three consecutive samples have exceeded the threshold values. Thus, a fault occurrence is detected by algorithm of Fig. 6.

After detecting a fault, fault location algorithm is activated based on Fig. 7. Based on this algorithm, and due to the positive sign of passing current in two modules 5 and 6, the fault location is determined on line 3.

After detecting the fault and its exact location, the fault identification algorithm is activated. Since the voltage drop in module 5 is more than module 6, so per unit pole-to-pole voltage in module 5 is investigated. Since it is 0.084 p.u and is less than 0.5 p.u, so based on Eq. 4, the occurred fault is a pole-to-pole one. It is observed that the proposed triple methods can detect pole-to-pole fault occurrence in line 3 of sample DC microgrid in Fig. 9.

**Table 2** Measured parameters by the modules of Fig. 9 before and after fault $F1$

| Module number | Number of samples | $V_{p.u}^{m}$ | | $CA_{p.u}^{m}$ | | $CD_{p.u}^{m}$ | | Is the fault detected? |
|---|---|---|---|---|---|---|---|---|
| | | Before | After | Before | After | Before | After | |
| 1 | 1 | 1.038613 | 0.138056 | 1.011985 | 2.62737 | 0 | 0 | No |
| | 2 | | 0.139219 | | 2.823302 | | 0 | |
| | 3 | | 0.143531 | | 2.977002 | | 0 | |
| 2 | 1 | 0.953654 | 0.221119 | 1.011985 | 2.62737 | 0 | 0 | No |
| | 2 | | 0.240469 | | 2.823302 | | 0 | |
| | 3 | | 0.272375 | | 2.977002 | | 0 | |
| 3 | 1 | 0.953654 | 0.221119 | 0.971061 | 2.495113 | 0 | 0 | No |
| | 2 | | 0.240469 | | 2.665099 | | 0 | |
| | 3 | | 0.272375 | | 2.804499 | | 0 | |
| 4 | 1 | 0.97696 | 0.081212 | 0.971061 | 2.495113 | 0 | 0 | No |
| | 2 | | 0.083203 | | 2.665099 | | 0 | |
| | 3 | | 0.091602 | | 2.804499 | | 0 | |
| 5 | 1 | 0.97696 | 0.081212 | 1.052909 | 2.362856 | 0 | 5.600643 | Yes |
| | 2 | | 0.083203 | | 2.506897 | | 6.060363 | |
| | 3 | | 0.091602 | | 2.699597 | | 6.399763 | |
| 6 | 1 | 0.97696 | 0.105811 | 1.052909 | 3.237787 | 0 | 5.600643 | Yes |
| | 2 | | 0.10125 | | 3.553466 | | 6.060363 | |
| | 3 | | 0.12075 | | 3.700166 | | 6.399763 | |
| 7 | 1 | 1.040266 | 0.105811 | 0.889213 | 2.098342 | 0 | 0 | No |
| | 2 | | 0.10125 | | 2.190493 | | 0 | |
| | 3 | | 0.12075 | | 2.307193 | | 0 | |
| 8 | 1 | 1.038613 | 0.138056 | 0.889213 | 2.098342 | 0 | 0 | No |
| | 2 | | 0.139219 | | 2.190493 | | 0 | |
| | 3 | | 0.143531 | | 2.307193 | | 0 | |

#### 4.1.2 Asymmetric Fault Detection

To investigate the proposed method ability to detect an asymmetric fault, a high impedance pole-to-ground fault with fault resistance of 0.01 is located in point $F2$ of microgrid of Fig. 9. Table 3 shows the recorded values by different modules before and after fault $F2$.

The results of Table 3 show that there is a fault in the network. Since based on fault occurrence, the recorded values exceed the threshold values in modules 3 and 4. In fact, different values measured after the occurrence of a fault in different modules show that all measured values for all three parameters of $V_{p.u}^{m}$, $CA_{p.u}^{m}$ and $CD_{p.u}^{m}$ and for all three measure samples in the third and fourth modules have surpassed their relevant thresholds which are, respectively, 0.8 p.u, 1.5 p.u and 2 p.u. Therefore, according to the suggested algorithm for fault detection, this is correctly recognized by the mentioned modules as a fault.

Using fault location algorithm and due to the positive sign of current of modules 3 and 4, the fault location is on line 2.

To determine the fault type, since voltage drop in module 3 is more than module 4, and also since the voltage is 0.6 p.u and pole-to-ground voltage amplitude in positive and negative poles are 0.5 and 1 p.u, respectively, hence based on Eq. 4, the type of the fault is negative pole-to-ground fault. Therefore, it is observed that the occurred fault is detected correctly in line 2 of sample DC microgrid based on the proposed triple algorithms.

#### 4.1.3 Evaluation of the Proposed Method in Detecting Switching Transient

To evaluate the proposed method reliability against transient states due to switching, the behavior of the fault detection algorithm is investigated during the outage of load 2.

Parameters values which are recorded by modules during mentioned switching transient are presented in Table 4. Investigating this table shows that none of the modules have detected any fault. So, the proposed method can

**Table 3** Measured parameters by modules of Fig. 9 before and after fault $F2$

| Module number | Number of samples | $V^m_{p.u}$ | | $CA^m_{p.u}$ | | $CD^m_{p.u}$ | | Is the fault detected? |
|---|---|---|---|---|---|---|---|---|
| | | Before | After | Before | After | Before | After | |
| 1 | 1 | 1.038613 | 0.666445 | 1.011985 | 2.607924 | 0 | 0 | No |
| | 2 | | 0.680439 | | 2.610867 | | 0 | |
| | 3 | | 0.702651 | | 2.62816 | | 0 | |
| 2 | 1 | 0.953654 | 0.58813 | 1.011985 | 2.607924 | 0 | 0 | No |
| | 2 | | 0.600387 | | 2.610867 | | 0 | |
| | 3 | | 0.611532 | | 2.62816 | | 0 | |
| 3 | 1 | 0.953654 | 0.58813 | 0.971061 | 2.221317 | 0 | 4.401522 | Yes |
| | 2 | | 0.600387 | | 2.23187 | | 4.421629 | |
| | 3 | | 0.611532 | | 2.232793 | | 4.424688 | |
| 4 | 1 | 0.97696 | 0.63832 | 0.971061 | 2.180205 | 0 | 4.401522 | Yes |
| | 2 | | 0.640413 | | 2.189759 | | 4.421629 | |
| | 3 | | 0.669719 | | 2.191895 | | 4.424688 | |
| 5 | 1 | 0.97696 | 0.63832 | 1.052909 | 2.441415 | 0 | 0 | No |
| | 2 | | 0.640413 | | 2.442424 | | 0 | |
| | 3 | | 0.669719 | | 2.449586 | | 0 | |
| 6 | 1 | 1.040266 | 0.747464 | 1.052909 | 2.441415 | 0 | 0 | No |
| | 2 | | 0.76049 | | 2.442424 | | 0 | |
| | 3 | | 0.790394 | | 2.449586 | | 0 | |
| 7 | 1 | 1.040266 | 0.747464 | 0.889213 | 1.845495 | 0 | 0 | No |
| | 2 | | 0.76049 | | 1.852873 | | 0 | |
| | 3 | | 0.790394 | | 1.85625 | | 0 | |
| 8 | 1 | 1.038613 | 0.666445 | 0.889213 | 1.845495 | 0 | 0 | No |
| | 2 | | 0.680439 | | 1.852873 | | 0 | |
| | 3 | | 0.702651 | | 1.85625 | | 0 | |

distinguish the permanent faults and transient states of the network properly.

### 4.2 Fault Detection in DC Microgrid in Network-Connected Mode

In the second case of the simulation, the proposed triple methods are investigated in DIgSILENT software for a network-connected microgrid. The studies of this section are implemented on a sample DC microgrid shown in Fig. 10 which has been used in Salomonsson et al. (2009). As presented in this figure, there is a converter in sample microgrid that connects AC part to DC microgrid and a set of battery and two set of loads which are connected to the DC bus via two lines.

**Table 4** Measured parameters by modules of Fig. 9 before and after the outage of load 2

| Module number | $V^m_{p.u}$ | | $CA^m_{p.u}$ | | $CD^m_{p.u}$ | | Is the fault detected? |
|---|---|---|---|---|---|---|---|
| | Before | After | Before | After | Before | After | |
| 1 | 1.038613 | 1.142474 | 1.011985 | 0.911698 | 0 | 0 | No |
| 2 | 0.953654 | 1.096702 | 1.011985 | 0.911698 | 0 | 0 | No |
| 3 | 0.953654 | 1.096702 | 0.971061 | 0.80253 | 0 | 0 | No |
| 4 | 0.97696 | 1.172352 | 0.971061 | 0.80253 | 0 | 0 | No |
| 5 | 0.97696 | 1.172352 | 1.052909 | 0.856023 | 0 | 0 | No |
| 6 | 1.040266 | 1.227513 | 1.052909 | 0.856023 | 0 | 0 | No |
| 7 | 1.040266 | 1.227513 | 0.889213 | 0.760011 | 0 | 0 | No |
| 8 | 1.038613 | 1.142474 | 0.889213 | 0.760011 | 0 | 0 | No |

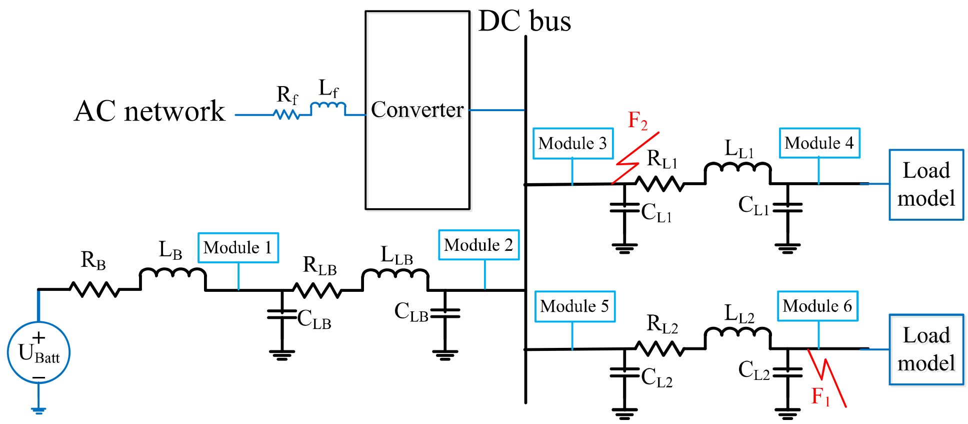


**Fig. 10** DC microgrid to evaluate the proposed method in network-connected mode

Considering the worst situation that can challenge the proposed method, the threshold values of $V^{m,\mathrm{TH}}$, $\mathrm{CA}^{m,\mathrm{TH}}$, and $\mathrm{CD}^{m,\mathrm{TH}}$ for various modules are acquired to be 0.8 p.u, 1.5 p.u, and 1.5 p.u, respectively.

#### 4.2.1 Pole-to-Pole Fault Detection

A pole-to-pole fault with insignificant fault resistance is put in the point $F1$ of sample microgrid of Fig. 10. Table 5 shows the electrical parameters measured by grid modules before and after this fault occurrence. Based on the presented results, a fault is recorded by module 5.

After detecting a fault occurrence, the fault location algorithm is activated. Since both modules 5 and 6 have the most voltage drop and their passing current sign is positive, the fault location is determined on line 2. Since the voltage drop in module 6 is more than module 5, per unit value of pole-to-pole voltage of module 6 is investigated. This voltage value is 0.047 p.u and is less than 0.5 p.u, so the occurred fault is a pole-to-pole one based on the proposed algorithm of Fig. 8.

**Table 5** Measured parameters by modules of Fig. 10 before and after fault $F1$

| Module number | Number of samples | $V^m_{\mathrm{p.u}}$ | | $\mathrm{CA}^m_{\mathrm{p.u}}$ | | $\mathrm{CD}^m_{\mathrm{p.u}}$ | | Is the fault detected? |
|---|---|---|---|---|---|---|---|---|
| | | Before | After | Before | After | Before | After | |
| 1 | 1 | 0.984937 | 0.346236 | 1.080246 | 2.052877 | 0 | 0 | No |
| | 2 | | 0.367338 | | 2.217345 | | 0 | |
| | 3 | | 0.404106 | | 2.427683 | | 0 | |
| 2 | 1 | 0.983456 | 0.152417 | 1.080246 | 2.052877 | 0 | 0 | No |
| | 2 | | 0.174349 | | 2.217345 | | 0 | |
| | 3 | | 0.236585 | | 2.427683 | | 0 | |
| 3 | 1 | 0.983456 | 0.152417 | 0.949947 | 0.225534 | 0 | 0 | No |
| | 2 | | 0.174349 | | 0.258482 | | 0 | |
| | 3 | | 0.236585 | | 0.298225 | | 0 | |
| 4 | 1 | 0.982161 | 0.064922 | 0.949947 | 0.225534 | 0 | 0 | No |
| | 2 | | 0.076305 | | 0.258482 | | 0 | |
| | 3 | | 0.112545 | | 0.298225 | | 0 | |
| 5 | 1 | 0.983456 | 0.152417 | 0.852517 | 2.744838 | 0 | 2.814004 | Yes |
| | 2 | | 0.174349 | | 2.974526 | | 3.063036 | |
| | 3 | | 0.236585 | | 3.145722 | | 3.266913 | |
| 6 | 1 | 0.981606 | 0.04253 | 0.852517 | 0.069166 | 0 | 2.814004 | No |
| | 2 | | 0.046631 | | 0.08851 | | 3.063036 | |
| | 3 | | 0.080591 | | 0.12119 | | 3.266913 | |

**Table 6** Measured parameters by the modules of Fig. 10 before and after the fault $F2$

| Module number | Number of samples | $V^m_{p.u}$ | | $CA^m_{p.u}$ | | $CD^m_{p.u}$ | | Is the fault detected? |
|---|---|---|---|---|---|---|---|---|
| | | Before | After | Before | After | Before | After | |
| 1 | 1 | 0.984937 | 0.723332 | 1.080246 | 1.143988 | 0 | 0 | No |
| | 2 | | 0.747992 | | 1.163494 | | 0 | |
| | 3 | | 0.765214 | | 1.196539 | | 0 | |
| 2 | 1 | 0.983456 | 0.610443 | 1.080246 | 1.143988 | 0 | 0 | No |
| | 2 | | 0.620734 | | 1.163494 | | 0 | |
| | 3 | | 0.636024 | | 1.196539 | | 0 | |
| 3 | 1 | 0.983456 | 0.610443 | 0.949947 | 1.714897 | 0 | 1.793426 | Yes |
| | 2 | | 0.620734 | | 1.721965 | | 1.810271 | |
| | 3 | | 0.636024 | | 1.789932 | | 1.908534 | |
| 4 | 1 | 0.982161 | 0.506584 | 0.949947 | 0.078529 | 0 | 1.793426 | No |
| | 2 | | 0.513873 | | 0.088306 | | 1.810271 | |
| | 3 | | 0.52598 | | 0.118602 | | 1.908534 | |
| 5 | 1 | 0.983456 | 0.610443 | 0.852517 | 0.416388 | 0 | 0 | No |
| | 2 | | 0.620734 | | 0.441529 | | 0 | |
| | 3 | | 0.636024 | | 0.474949 | | 0 | |
| 6 | 1 | 0.981606 | 0.499715 | 0.852517 | 0.416388 | 0 | 0 | No |
| | 2 | | 0.505267 | | 0.441529 | | 0 | |
| | 3 | | 0.509307 | | 0.474949 | | 0 | |

#### 4.2.2 Positive Pole-to-Ground Faults Detection

In this part of simulations, a positive pole-to-ground fault with 5 mΩ fault resistance is put at point $F2$ of microgrid of Fig. 10. Table 6 shows measured parameters before and after this fault.

Investigating the results shows that a fault is identified by module 3. The fault current direction analysis shows that the sign of current of modules 3 and 4 was positive. Therefore, the fault location is determined to be on line 1. In addition, since the voltage drop in module 4 is more than module 3, and since its value is more than 0.5 p.u, and line-to-ground voltage amplitude in positive and negative poles are 0.02 p.u and 0.5 p.u, the fault is identified to be a positive pole-to-ground fault.

## 5 Conclusion

In this article, three algorithms are presented to detect a fault, determine its exact location, and also determine its type and characterization. The proposed algorithms are based on sampled values of voltage and current signals of different points of the network. Acquired results of implementing the proposed triple methods on two sample microgrids in the islanded and connected to grid modes show that the proposed methods have capability in fault detection processes, location, and identification of its type properly. In addition, the proposed methods can appropriately respond to structural uncertainties of microgrid. Other abilities of the proposed method are that by analyzing voltage and current signals of different points of the network, as shown in the simulation results, the proposed fault detection method can distinguish permanent faults from network transient state such as switching.

## References


Abdali A et al (2017) Fast fault detection and isolation in low-voltage DC microgrids using fuzzy inference system. In: 5th Iranian joint congress on fuzzy and intelligent systems (CFIS). pp 172–177

Abdali A et al (2019) Simultaneous control and protection schemes for DC multi microgrids systems. Int J Electr Power Energy Syst 104:230–245

Amamra S-A et al (2017) Firefly algorithm optimized robust protection scheme for DC microgrid. Electr Power Compon Syst 45:1141–1151

Aswani J, Kanakasabapathy P (2016) Protection of a low-voltage DC ring microgrid system. In: International conference on energy efficient technologies for sustainability (ICEETS). pp 17–22

Balasreedharan SS, Thangavel S (2016) An adaptive fault identification scheme for DC microgrid using event based classification. In: 3rd international conference on advanced computing and communication systems (ICACCS). pp 1–7

Basak P et al (2012) A literature review on integration of distributed energy resources in the perspective of control, protection and stability of microgrid. Renew Sustain Energy Rev 16:5545–5556

Conti S (2009) Analysis of distribution network protection issues in presence of dispersed generation. Electr Power Syst Res 79:49–56

Conti S, Nicotra S (2009) Procedures for fault location and isolation to solve protection selectivity problems in MV distribution networks with dispersed generation. Electr Power Syst Res 79:57–64

Dhar S, Dash PK (2017) Differential current-based fault protection with adaptive threshold for multiple PV-based DC microgrid. IET Renew Power Gener 11:778–790

Dhar S et al (2018) Fault detection and location of photovoltaic based DC microgrid using differential protection strategy. IEEE Trans Smart Grid 9:4303–4312

Eslami R et al (2017a) A probabilistic approach for the evaluation of fault detection schemes in microgrids. Eng Technol Appl Sci Res 7:1967–1973

Eslami R et al (2017b) A novel method for fault detection in future renewable electric energy delivery and management microgrids, considering uncertainties in network topology. Electr Power Compon Syst 45:1118–1129

Hosseini SA et al (2016) An overview of microgrid protection methods and the factors involved. Renew Sustain Energy Rev 64:174–186

Hosseini SA et al (2018a) Improving adaptive protection to reduce sensitivity to uncertainties which affect protection coordination of microgrids. Iran J Sci Technol Trans Electr Eng 42:63–74

Hosseini SA et al (2018b) A decision-tree scheme for responding to uncertainties in microgrid protection coordination. Electr Power Compon Syst 46:1–14

Howlader A et al (2018) Design and line fault protection scheme of a DC microgrid based on battery energy storage system. Energies 11:1823–1845

Jae-Do P et al (2013) DC ring-bus microgrid fault protection and identification of fault location. IEEE Trans Power Deliv 28:2574–2584

Jamali SZ et al (2018) A high-speed fault detection, identification, and isolation method for a last mile radial LVDC distribution network. Energies 11:2901

Lv C et al (2018) Single-ended protection scheme for VSC-based DC microgrid lines. Energies 11:1440–1457

Maqsood A, Corzine K (2016) DC microgrid protection: using the coupled-inductor solid-state circuit breaker. IEEE Electr Mag 4:58–64

Meghwani A et al (2017) A non-unit protection scheme for DC microgrid based on local measurements. IEEE Trans Power Deliv 32:172–181

Ming Y et al (2016) DC short circuit fault analysis and protection of ring type DC microgrid. In: IEEE 8th international power electronics and motion control conference. pp 1694–1700

Mohanty R, Pradhan AK (2017) Protection of smart DC microgrid with ring configuration using parameter estimation approach. IEEE Trans Smart Grid 9:1

Mohanty R, Pradhan AK (2018) DC ring bus microgrid protection using the oscillation frequency and transient power. IEEE Syst J 13:1–10

Nimpitiwan N et al (2007) Fault current contribution from synchronous machine and inverter based distributed generators. IEEE Trans Power Deliv 22:634–641

Park JD, Candelaria J (2013) Fault detection and isolation in low-voltage DC-bus microgrid system. IEEE Trans Power Deliv 28:779–787

Salomonsson D et al (2009) Protection of low-voltage DC microgrids. IEEE Trans Power Deliv 24:1045–1053

Shabani A, Mazlumi K (2019) Evaluation of a communication-assisted overcurrent protection scheme for photovoltaic based DC microgrid. IEEE Trans Smart Grid. https://doi.org/10.1109/TSG.2019.2923769

Shehzad Hassan MA et al (2018) Microgrid control and protection state of the art: a comprehensive overview. J Electr Syst 14:148–164

Wen H, Weiqiang Z (2016) Control and protection of DC microgird with battery energy storage system. In: IEEE international conference on power electronics, drives and energy systems (PEDES). pp 1–6

Zhao Z et al (2016) Hierarchical coordinated control of multi bus-based DC microgrid considering fault occurred in buses. In: China international conference on electricity distribution (CICED). pp 1–6